SYNTHESIS AND PHOTOSTABILITY STUDIES OF FUNCTIONALIZED LUMINESCENT SEMICONDUCTOR PARTICLES.

Advisor: Prof. B. Dragnea

Name: Nancy Goicochea

INTRODUCTION

Nowadays, the understanding of intracellular processes, signal transduction and protein-protein interactions has improved thanks to the utilization of more efficient fluorescent probes.[1] The unique properties of nanoparticles make nanoparticle-biomaterial conjugates attractive probes for sensing applications. Semiconductor nanoparticles Quantum Dots (QD) are an example of nanoparticles with attractive spectroscopic properties.[2] QD's offer many advantages compared to fluorophores, commonly used in fluorescence microscopy. Quantum dots are nanocrystals of a few nanometers in diameter. Their different size and shape depends on the temperature, surfactant and duration of the synthesis. This produces quantum dots with size-dependent tunable optical properties.[1,2] If the light shined on the semiconductor nanoparticles has higher photon energy than the band gap energy, then an electron-hole pair is created. Thus, it results in a broad absorption spectrum, compared to fluorophores, which possess a narrow absorption spectrum. Electron pair recombination results in a narrow emission peak.[1] The maximum emission wavelength is shifted to lower energies (red shifted) as the particle size increase, due to quantum confinement effects.[3] However, defects on the surface of the nanocrystal produce traps that account for losses in the fluorescence. This effect causes a great diminution in the quantum yield (QY), which stands for number of emitted photons over adsorbed photons. [1] One way to eliminate these carrier traps is to passivate the surface of

the nanocrystal by coating it with a material of a larger energy band gap. After this treatment, many of the surface traps disappear, increasing the QY and the fluorescence lifetime up to several hours,[4] in contrast to common dyes, which possess small lifetimes (in the submicrosecond to millisecond range). Moreover, the surface properties can be precisely changed to match different specific applications. In particular, the nanoparticles can be coated with a hydrophilic layer to use them as sensors in biological systems.[1]

QD's are commonly synthesized in non-polar organic solvents, therefore their surface needs to be functionalized in order to be compatible with biological environments. In particular, two important strategies to prepare water-soluble nanocrystals are going to be discussed in the following lines. One approach deals with QD's nanocrystals attached to streptavidin directly through an active ester coupling reaction. This produces nanocrystals with streptavidin covalently attached on the surface, 5-10 streptavidins per QD conjugate, which results in QD's Streptavidin Conjugates (QD-SAV) with specific biological activity.[5,6] For example, QD-SAV can be bioconjugated to biotynilated proteins for biological labeling.[1]

Recent developments deal with the encapsulation of QD's inside phospholipid micelles through hydrophobic-hydrophilic interactions.[7] This process provides a

biological layer soluble in aqueous media. Moreover, the selection of the lipid can be such to make the QD's specific biocompatible probes[7].

OBJECTIVES

Due to the extraordinary optical properties of QD, they are useful tools for biological applications. In particular, it is aimed to design biocompatible, photostable biosensor QD's to be incorporated inside viral capsid (Brome Mosaic Virus) in order to track intracellular viral pathways via spectroscopic methods. As a result this research project has been divided in the following targets given below:

I Modify the surface layer of quantum dots to provide a photostable biological interface to incorporate them inside the virus capsid, which in turn will be used as the carrier of these photoluminescent probes. Two modifications are proposed:

a) Micelle phospholipids incorporated inside quantum dots[7] of the appropriate size for the viral capsid. Refer to **figure 1.**

b) QD-streptavidin conjugate attached to a single strand of biotynilated DNA, with the appropiate sequence to ensure compatibility with the viral capsid genetic material. Refer to **figure 1.**

II Perform photostability studies[9] of the biocompatible nanoprobes to determine their stability under laser exposure. In particular, it is targeted to determine which coating shell (biotin-avidin or micelle phospholipids) is more effective in preventing photoannealing and photodegradation of the nanoparticles as a consequence of the interaction between the core of the quantum dots (CdSe/ZnS) and the reactive species from the aqueous media or the environment. Refer to **figure 1.**

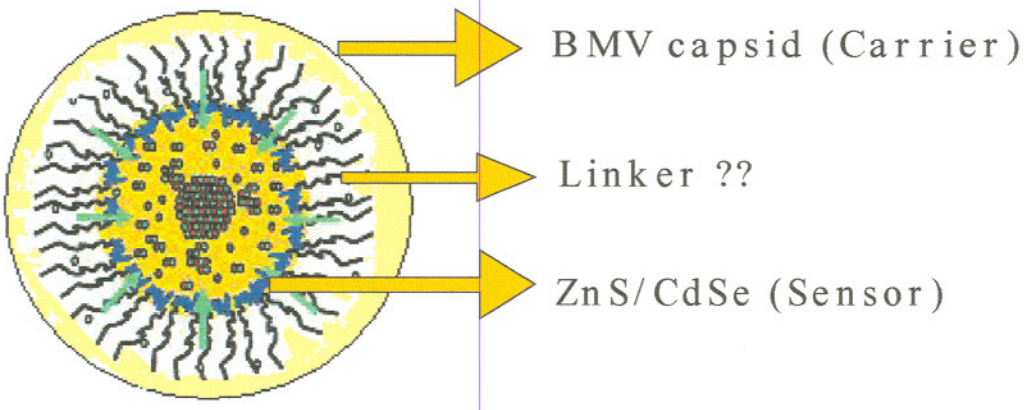

Figure 1. The big picture: Surface modified Quantum Dots (optical nanoprobe) incorporated inside Brome Mosaic (BMV) viral capsid.

LITERATURE REVIEW

Semiconductor quantum dots are of interest due to their optical properties. Among other materials, CdSe colloids are the most studied due to their fluorescence emission in the visible range and their eminent use in material science, biotechnology and biology.[10] To use semiconductor nanoparticles as optical probes, it is necessary to account for the energy requirements. The total charging energy of semiconductor QD's is obtained from the direct Coulomb interactions between the charges of the nanocrystal and from the polarization energy, which depends on the shape and size of the semiconductor. The energy band gap of QD's can varies with the dielectric media due to interactions of the exciton with the surface polarization charge.[11] In particular, the dielectric forces are also important in the case of surface functionalized QD's. The optical band gap can be accurately calculated, if the shell coating is taken in consideration. The exciton total energy contained in a spherical nanocrystal is the result of the sum of the bulk band gap, the kinetic energy of each electron-hole pair, the Coulomb interactions derived from the electron-hole system, the self – charging energy of each carrier, $\sum_{e(h)}^{pol}$, and the polarization energy as a result of electrostatic interaction between species of opposite charge, $J_{e,h}^{pol}$.[11] See equation **1.**

$$E_{gap}^{opt} = E_g^{bulk} + E_e^{kin} + E_{hole}^{kin} + E_{Coul}^{ir} + \sum_{hole}^{pol} + \sum_{e}^{pol} + J_{e,h}^{pol} \quad \textbf{(1)}$$

The energy terms from equation **1** accounts for the dielectric constant inside the QD's (ε1). The last three polarization terms depend on the external dielectric surroundings (ε3). In the presence of an electric field, the layer between the charges inside the core and the external environment becomes charged. Thus, after few corrections in the exciton energy, to account for the interaction between an spherical QD core (ε1) and a shell of a second material with dielectric constant ε2 an thickness (b-a) and immersed in different dielectric solvent (ε3), as shown in **figure 2**. All these modifications are expressed in equation (**2**)[11]:

$$\delta = \frac{\pi q^2}{2\varepsilon_0 \varepsilon_1 a} \sum_{l=1}^{\infty} a^{2l+1} A_l \int_0^1 j_0^2(\pi x) x^{2l+2} \partial x \quad \textbf{(2)}$$

In equation **2**, ε0 is the permittivity at vacuum, is the QD radius, q is a point charge at position r' inside a spherical region and j_0^2 represents the spherical Bessel function. In this case A_l is given by[11]:

$$A_l = \frac{(l+1)a^{2l+1}(\varepsilon_2 - \varepsilon_3)[\varepsilon_1 + l(\varepsilon_1 + \varepsilon_2)] + b^{2l+1}(\varepsilon_1 - \varepsilon_2)[\varepsilon_3 + l(\varepsilon_2 + \varepsilon_3)]}{a^{2l+1}a^{2l+1}(\varepsilon_1 - \varepsilon_2)(\varepsilon_2 - \varepsilon_3)l(l+1) + b^{2l+1}[\varepsilon_2 + l(\varepsilon_1 + \varepsilon_2)][\varepsilon_3 + l(\varepsilon_2 + \varepsilon_3)]} \quad \textbf{(3)}$$

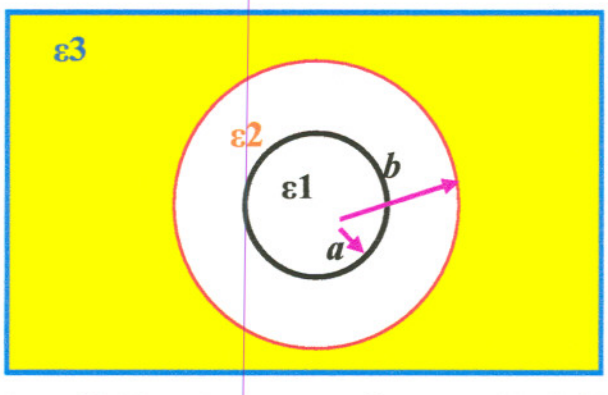

Figure 2. Distribution of Dielectric constants for a core/shell QD (ε1, ε2) in a dielectric medium.

After accounting for the energy requirements to excite the quantum dots, now the discussion will be focused in the stability and optical properties of photoexcited colloidal semiconductor nanoparticles dispersed in solution.

In the case of core/shell quantum dots, such as CdSe/ ZnS, it is believed that the thickness of the shell is directly related to the luminescence quantum yield (QY), since many of the surface traps are now eliminated by the outer layer. Even though, this system is not perfect and typically the QY for core/shell dots are in the 1-10 % range.[4] However, when core/shell nanoparticles are exposure to UV light in the presence of air, the QY increases dramatically as a consequence of a structural reorganization of the shell induced by the laser light.[10,12] The proposed reaction mechanism involves the adsorption of oxygen and/or water molecules on the surface, which reduces the changes of recombination from the shell energy

traps or photooxidation in the surface. Moreover, after a long period of photoirradiation, photooxidation takes place, as shown in **figure 3**. The QY from annealed core/shell nanoparticles remains high even for several months.[10]

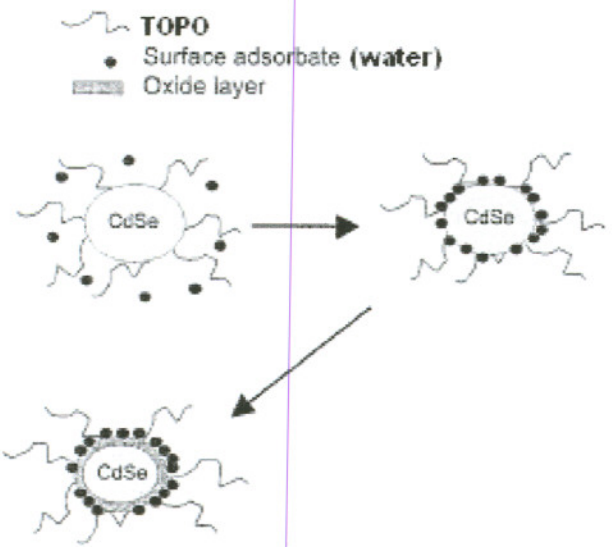

Figure 3. Proposed adsorption model for the photoannealing of core/shell QD in presence of air.[10]

The dependence on CdSe QD size (from 2.8 nm to 6 nm) is shown in **figure 4a**. All the three curves fit well with a biexponential rise and a single exponential decay. The exponential decay constant is largest for the smallest QD size and smallest for the largest QD. In **figure 4b**, the integrated intensity versus the illumination time in air of TOP/TOPO coated quantum dots (CdSe/ZnS) is presented. The curve fit with a biexponential rise.

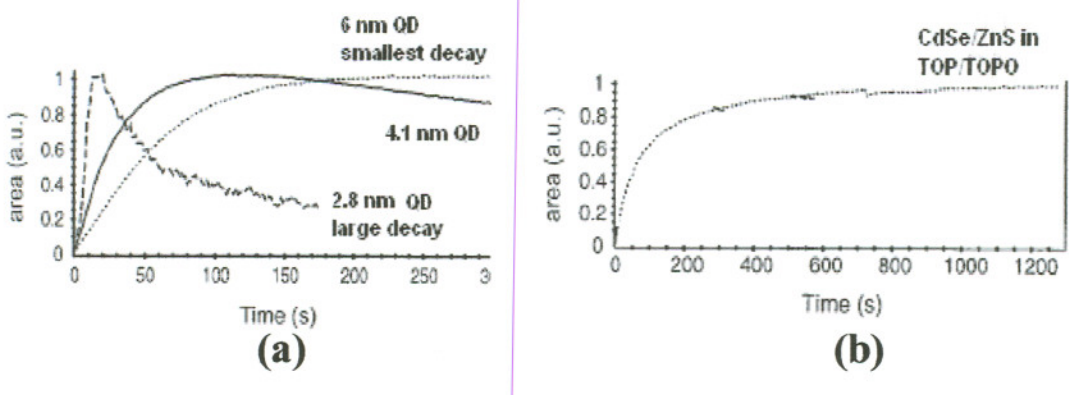

Figure 4. Graph (a) shows the luminescence intensity for 2.8 nm QD (dashed line), 4.1 nm QD (solid line) and 6 nm QD (dotted line). Graph (b) represents the integrated intensity for a 4.1 nm CdSe/ZnS QD's in TOP/TOPO.[10]

Despite the interest of Quantum Dots for biological imaging, it has been a tough job to meet the biological requirements. These include the solubilization of QD's in aqueous media at different pH, to maintain the optical properties of QD's in aqueous media, to overcome non-specificity adsorption and aggregation, and to account for cytotoxicity.[13]

Typically, biological experiments use fluorescent organic dyes or proteins as fluorescent probes. The problem is that even the best fluorescent dye has small fluorescent lifetimes and limits the monitoring of the live experiments.[7] To overcome this problem, nowadays organic dyes are being replaced by semiconductor nanocrystals, which exhibits high photostability, as discussed in the previous paragraphs[10, 14] and also the optical tunability of QDs allows to excite

different sizes of particles using a single excitation wavelength. Therefore, it is possible to use more than one semiconductor QD as optical probes simultaneously.[15]

One disadvantage of using semiconductor nanocrystals as synthesized is that the nanoparticles are produced from a hydrophilic environment.[5] Therefore, the non polar quantum dots need to be functionalized to be compatible with the biological media.

To obtain biocompatible QD, different strategies have been reported in the literature, including surface modification with thiolated ligands,[17] oligomeric phosphines,[18] dendromeric structures,[19] and peptides.[6, 20] Other approaches involve the encapsulation of QD's inside silica beats,[14] phospholipid micelles,[7] among others.

From all the strategies mentioned in the previous paragraph, only a few are adequate for our purposes. To construct a biosensor that can be incorporated inside Brome Mosaic Virus (BMV), the size of the optical probe should be no longer than 14 nm in diameter, since the BMV viral capsid has been determined to be 28 nm.[8] For this particular purpose, the micelle encapsulated QD's and the functionalization of QD's with streptavidin peptides are the most suitable option.

To couple QD's with peptides, a common procedure involves the covalent attachment of binding proteins to the QD's surface. In particular the avidin-biotin system is very well known for the high and specific interactions between this binding proteins due to the electrostatic interactions between the negatively charged streptavidin QD conjugate (SAV-QD) and the positively charged biotynilated ligand.[21] Typically 5 avidin are bound to the surface of the QD, but in practice, it is consider that there is only one streptavidin per QD. To ensure this ratio, the experiment should be carried out at saturation levels. In this way, biotynilated ligands can be easily attached to the surface of the QD through an avidin-biotin bridge.[21] One difficulty of this process is that the nanocrystals tend to aggregate and adsorb non specifically when used in biological environments,[7] refer to **figure 5a.**[20]

On the other hand, the micelle approach satisfies simultaneously many of the requirements of biological systems. The micelle shell functions as a protector of the inner structure of the QD's and provides the biological interface to act as bio-probes, it is also responsible for the solubilization in water while keeping the QD's optical properties, provides colloidal stability, and low non specific adsorption, refer to **figure 5b**[1, 7]

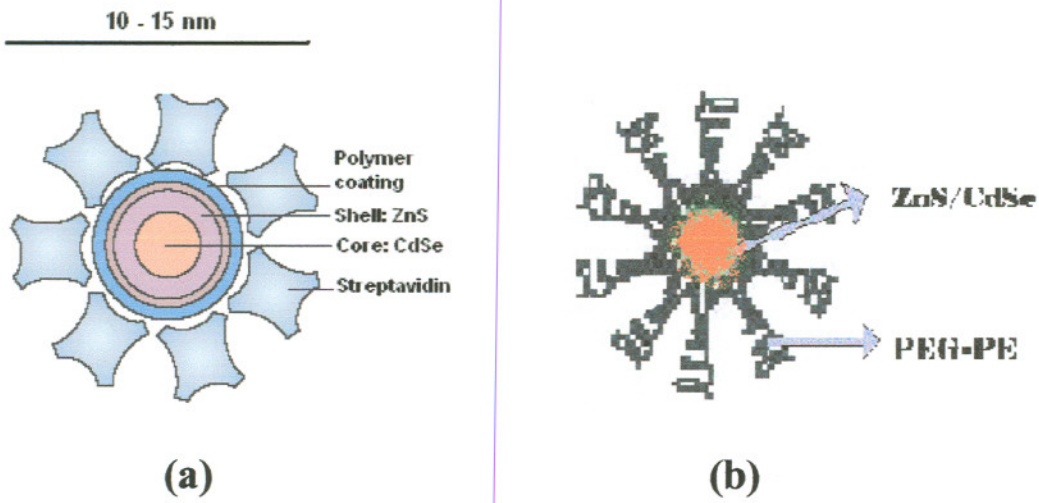

Figure 5. Functionalization of QD's. In part (a) the QD-SAV[20, 21] approach has been represented and in part (b) the micelle QD encapsulation[1,7] is schematized.

The micelle structure is composed of a hydrophobic core and a hydrophilic tale, the core can be composed of *n*-poly(ethyleneglycol) phosphatidylethanolamine (PEG-PE) or a mixture of phosphatidylcholine (PC) and PEG-PE, refer to **figure** . This combination is useful since PEG-PE allows for steric stabilization of PC liposomes.[22] PEG-PE's are classified as hydrophilic polymer grafted lipids,[7, 22] which in presence of water t hey self-assemble into micelles due to their amphiphilic nature. Typically, they assemble with the polar molecules (hydrophilic part) exposed to the water and the non-polar molecules (hydrophobic part) hidden in the core of the micelle. This transformation occurs only when the lipid concentration exceeds a critical micelle concentration (CMC),[23] refer to table **1.**[24] These macromolecules are commonly used for drug delivery due to their low

non specific adsorption and biocompatibility. These lipids can resemble the behavior of the cell membranes, that allows them to interact with specific targets on the surface of the cell or inside the cell membrane.[25]

Another advantage of using PEG- PE phospholipids to form micelles is due to their size flexibility and regular structure. The length of the hydrophilic PEG tail ((**L**) in **figure 6**) can be selected to obtain different sizes of micelle-QD's,[7] as shown in table **1.** PEG-PE's sizes are commercially available in the range of 350 - 3000 Da. Moreover, the stability of the micelle mixture is directly related to the PEG-PE content and in particular to the length of PEG.[22]

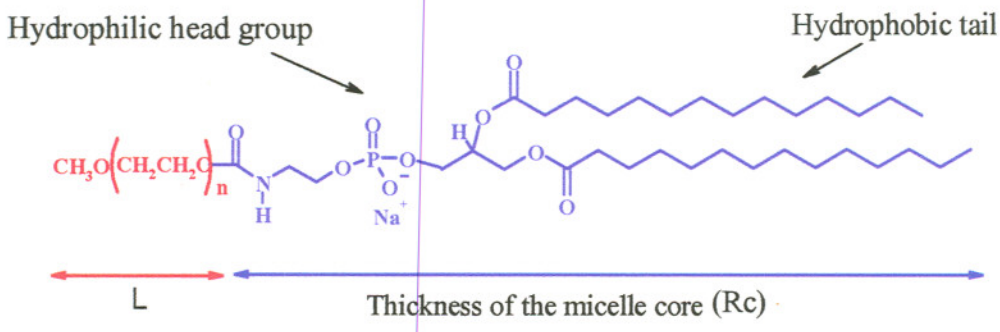

Figure 6. ***n*-poly(ethyleneglycol) phosphatidylethanolamine (PEG-PE)**

Table 1: Physical properties of some PEG-PE's[24]

PEG-X	$R_t = L + R_c$(Å)	R_c(Å)	L (Å)	CMC (uM)
750	51	34	17	4.9
2000	67	32	35	5
5000	107	32	75	4.8

From the discussion of these two QD surface modification procedures, the micelle-QD approach offers a more versatile option, since the possibility of adjusting the PEG length, provide us with a set of various lengths of phospholipid micelles, which can result in distinguishable photoreactivities and photobleaching phenomena. It is aimed to study the photostability of the micelle-QD's as a function of the PEG length in air. In particular, it is proposed to study if the lipid layer prevents the release of Cadmium ions (from the core of the QD's) to environment, and if so, which is the smallest PEG length that can effectively block these ions. This is an issue of importance, since the final goal is to incorporate the micelle-QD inside the viral capsid. For such a confined system, the release of few cadmium ions causes dramatic changes in the genetic material of the virus, the cys-cys bonds complex with the Cadmium ions, thus affecting the stability of the virus.

Another point to address is the photostability of SAV-QD compared to the micelle-QD's in aqueous media. Moreover, the PEG length will be adjusted to see if there any effect in the mobility of reactive species (H_2O, O_2) adsorbed in the surface of the QD's, originated from exposure of QD's to laser light.

EXPERIMENTAL WORK

The necessary steps to achieve the desired objectives of studying the photostability of micelle incorporated QD's is outlined in the following lines.

I. Synthetic Routes

1 Synthesis of Functionalized Quantum Dots. This is a two-step procedure, which requires first the preparation the semiconductor nanocrystal precursors using the protocol described elsewhere[16] and the second step addresses the biocompatibility through the phospholipid micelle encapsulation of QD's.[7]

2 Synthesis of QD-SAV conjugated to biotynilated DNA. This protocol involves the attachment of commercially available QD-SAV to a specific single DNA sequence through a simple procedure described elsewhere.[8]

II. Photostability Measurements

Photostability measurements on micelle-QD's containing different lengths of PEG's will allow to study the photochemistry of the surface of the QD, and to compare with the stability of the QD-SAV.

III. Characterization by Spectroscopy

Detection of QD's and functionalized QD's optical properties

Absorption Spectroscopy for the core/shell QD's

Fluorescence Spectroscopy (size distribution of QD's and derivatives)

Dynamic Light Scattering (quantitative size distribution)

Transmission Electron Microscopy (TEM) (particle size)

Gel Electrophoresis (to characterize charged nanoparticles)

I. Synthetic Routes

1. Synthesis of Functionalized Quantum Dots:

1.1 ***Synthesis of ZnS caped CdSe nanocrystals.***

PROCEDURE

The synthesis of ZnS-CdSe quantum dots proceeds following Hines and Guyot-Sionnest protocol.[16] This procedure was chosen among others due to its versatility, crystallinty and monodispersity of the particles that are obtained. This is a one pot reaction that allows producing CdSe core particles capped with a layer of ZnS.

This procedure involves the preparation of Cd and Zn stock solutions. Dimethyl cadmium (0.25 mL) is added to selenium pellets (0.2 g) previously dissolved in 4.5 mL of tri-n-octylphosphine (TOP) under argon atmosphere. The Cd stock solution is finally diluted with 19.5 mL of TOP. The Zn stock solution is prepared by adding dimethyl zinc (0.37 mL) to hexamethyldisilathiane (0.52 mL) in 4.5 mL of TOP and diluted with 19.5 mL of TOP.[16]

This approach requires drying and degassing of hot tri-n-octylphosphine oxide (TOPO) using a vacuum-argon line. After that, the temperature is increased to 250 °C keeping the Ar line. Once the temperature is stabilized, 0.7 mL of Cd/Se/TOP solution is injected and the temperature is allowed to cool down until 200 °C, at which temperature five 0.55 mL portions of ZnS/TOP solution is successively injected at a rate of 1drop/s. Finally, the temperature is allowed to cool until 100 °C and the reaction mixture is stirred during 1h. The nanoparticles are purified by precipitation with anhydrous methanol. The red pellet collected after centrifugation (3000 rpm) is dissolved in 10 mL of Chloroform. In this way, ZnS capped QD are produced with high stability and enhanced luminescence properties due to passivation.[16]

The typical Quantum Yield for ZnS/CdSe is reported in the literature to be 10 %. The experimental QY obtained is in agreement with the literature (8 %).

RESULTS AND DISCUSSION

The QD's synthesized by this method yielded dots of 4 nm in size (by TEM) and an emission band at 566 nm measured by Fluorescence spectroscopy, as shown in **figure 7**. To obtain good results, it is important to prepare fresh Cd stock solutions, since it goes rapid degradation. During the addition of ZnS/TOP solution it is required to observe the rate of 1 drop/s . This initiates the process of nucleation and allows the controlled growth of the nanocrystals. For a monodisperse sample, the nucleation has to be done in a short period of time and separated from the growth step. In contrast the growth step should be given enough time to produce a monodisperse distribution (1 drop per second).[26] If this ratio is not observed, the reaction tend to fail or a multidisperse distribution of sizes are obtained.

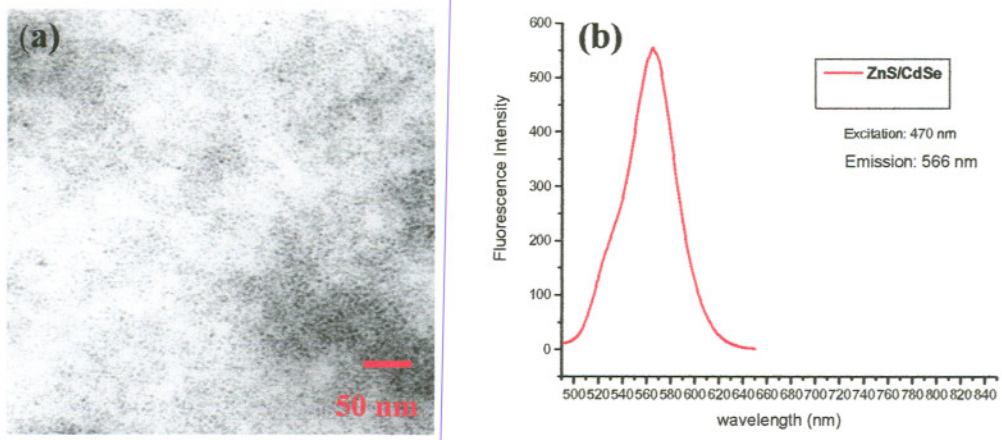

Figure 7. Characterization of ZnS/CdSe nanocrystals by TEM (a) and Fluorescence emission (b).

1.2 *Synthesis of PEG-PE micelle incorporated quantum dots.*

PROCEDURE

To address the problem of biocompatibility, Dubertret B and *et al*[7] came up with the idea to encapsulate semiconductor nanoparticles inside phospholipids micelles for *in vivo* experiments. The encapsulation of QD inside micelles goes trough a self-assemble process in presence of water. Powder PEG-PE (5.5 μmoles) is added to QD (2 mg) suspended in Chloroform (1 mL), and then the solvent is dried at vacuum. The reaction flask is placed in a water bath at 90 °C and the mixture is heated for three - four minutes to produce a reddish oily pellet that in presence of water (1 mL) forms an optically clear solution. After that, the solution is stirred at room temperature and sonicated. Ultracentrifugation at 90000 rpm during 2h at room temperature is used to isolate the empty micelles from those with QD inside[7]. After centrifugation a red pellet is collected and redisolved in water (1 mL). The synthetic route of this simple procedure is shown in **figure 8.**

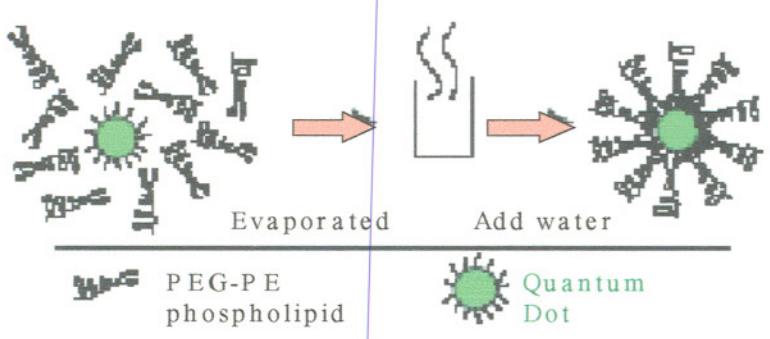

Figure 8. Scheme of the synthetic micelle approach

RESULTS AND DISCUSSION

The size of the micelle-QD's is characterized by TEM and Dynamic Light Scattering (DLS) (**figure 9a, 9b**) and the optical properties are corroborated by Fluorescence spectroscopy (**figure 9c**).

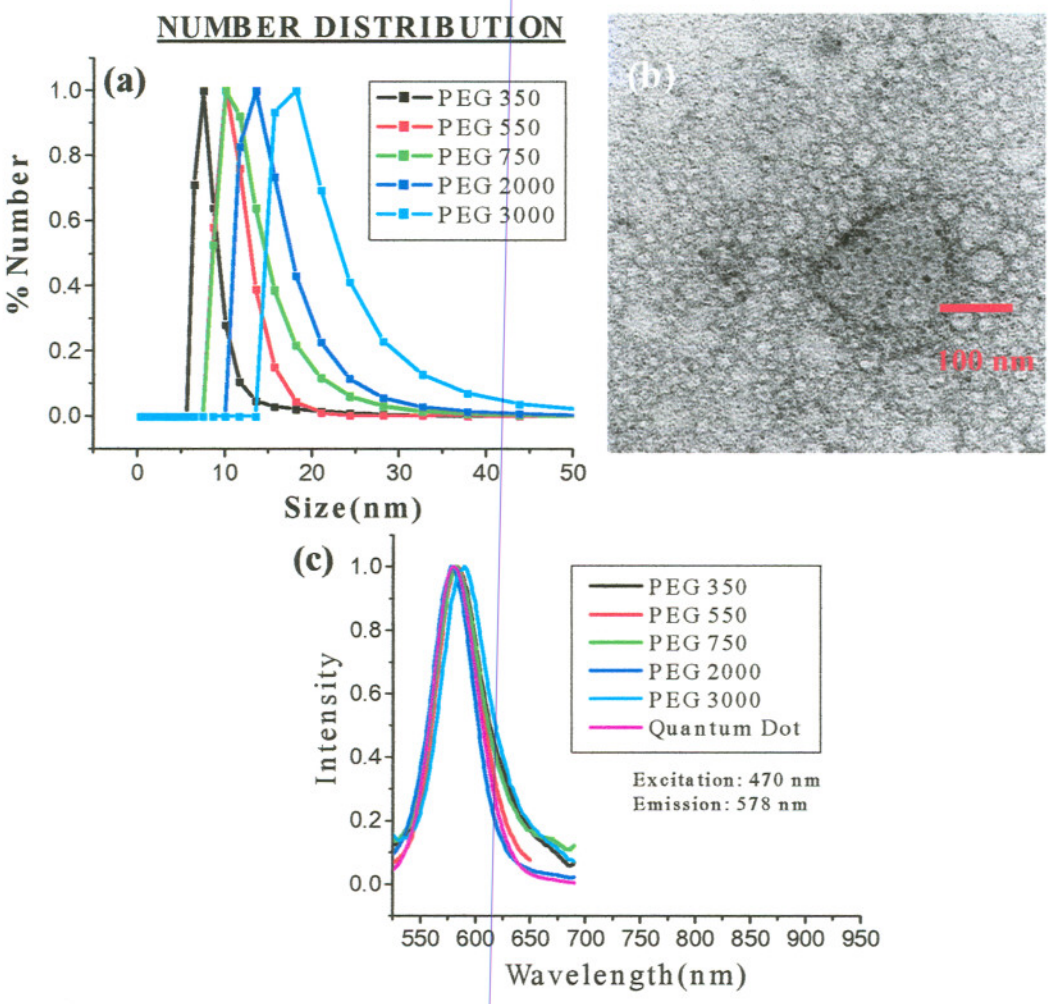

Figure 9. Characterization of the micelle-QD's. Part (a) represents the number distribution by DLS of 5 different sizes of micelle-QD; Part (b) shows the TEM negative stain of PEG-3000PE micelle-QD. Part (c) represents the fluorescent intensity for all the 5 studied systems.

To obtain accurate measurements of the size distribution by *Dynamic Light Scattering*, the micelle solution is diluted ten times and sonicated during several hours (5h) to prevent aggregation. After that, the sample is passed through a 100 nm filter connected to an injection, in such a way that any dust particle (> 100 nm) is trapped inside the filter and do not interfere with the size measurements. Another important consideration is that the size measurements should be taken per triplicate or more times to be reliable and special attention should be given to the correlation, which is the indicator of possible contamination in the sample.

The Number distribution measurements of the different micelle-QD's sizes revealed that the sizes of the dots are 7.5-8 nm for the PEG-350 PE micelle, 10-11 nm for the PEG-550 PE, 11.5-12 nm for the PEG-750 PE micelle, 14-17 nm for the PEG-2000 PE micelle, and 18-20 nm for the PEG-3000 PE micelle, as shown in **figure 9a**. For all the experiments the QD's particle size is about 4 nm, refer to **figure 7**.

The size characterization with *Transmission Electron Microscopy* (TEM) also requires a previous dilution of the sample, and sonication for several hours. A 10 μL drop containing the sample should be carefully deposited on the surface of a carbon coated cupper grid (200 mesh) and leave it for drying at room temperature for at least two hours. Typically the illumination power of the microscope is settled at 65 kV and the pictures are taken with a magnification of at least 150K to

be able to detect the QD's. Because of the nature of the phospholipid layer around the QD's, they are invisible to the electron beam unless the solution is stained. In this particular case, a solution of 1% PTA (Phosphotungstic acid), pH = 7 was selected. This is a commonly used acid for negative staining, since it makes the background to look darker than the sample and an inversion of the negative is required to see the lipidic coating clearly, as shown in **figure 9b.** A white spherical shell represents the phospholipids and the dark spots correspond to the QD's. With this technique, both micelle layer and QD's are visible at the same time.

In addition, the optical properties of the micelle quantum dots are corroborated by Fluorescence Spectroscopy. The results show that the phospholipid layer does not affect the dot energy levels, since the emission peak of the bare QD's and the encapsulated appears around the same value (578 nm), as shown in **figure 9c**, are in agreement with the literature.[5]

1.3 ***Synthesis of QD-SAV attached to biotynilated DNA.***

PROCEDURE

The avidin- biotin is a well known linker to attach nanoparticles to biotynilated proteins. Since both avidin and biotin are charged molecules, the strong

electrostatic interaction between these molecules accounts for rapid conjugation reactions[1, 5]

QD-SAV conjugates emitting at 605 nm (6μL, 1 μM), acquired from Quantum Dot Corporation, are mixed with an aqueous solution of biotynilated DNA (6 μL, 13 μM) and incubation buffer (6 μL, pH = 8.4). The single stranded DNA sequence is chosen, so that it can be recognized by the BMV viral capsid.[8]

The chosen ssDNA strand is composed of 30 bases and is 10 nm long, with its 5' terminus attached to biotin, and it is selected using the following sequence: 5'Bio/GTC TTC CGCTCTCGGCAGAGGTGTGAAGGA-3'[8]. The mixture is stirred for 30 minutes at room temperature.

Confirmation of the DNA attachment with the QD's is followed by Gel Electrophoresis. To see clearly the movement of the avidin-biotin system, a concentrated sample is needed. The matrix is made of agarose gel (2%) and the liquid phase is provided by TBE buffer (TRIS base (0.4 M), Boric acid (0.45 M), EDTA (10 mM)). The reference and the sample (10 - 20 μL) are inserted in the small holes made in the gel. The voltage is set to run from negative to positive poles, the power is 75 mV. After 2 h of running the experiment, the QD-SAV/BIO-DNA conjugated moves around 1 cm with respect to the reference (QD-SAV), see **figure 10a.** This experiment represents an evidence of avidin-biotin attachment and that the QD remains attached to the streptavidin, which is achieved by following the reaction under UV light. Dynamic Light Scattering is

used to account for the final size of the QD-DNA bioconjugate. The initial size of the QD-SAV found under DLS was 13.54 nm, while the size of QD-DNA conjugate was 18.17 nm as shown in **figure 10b.**

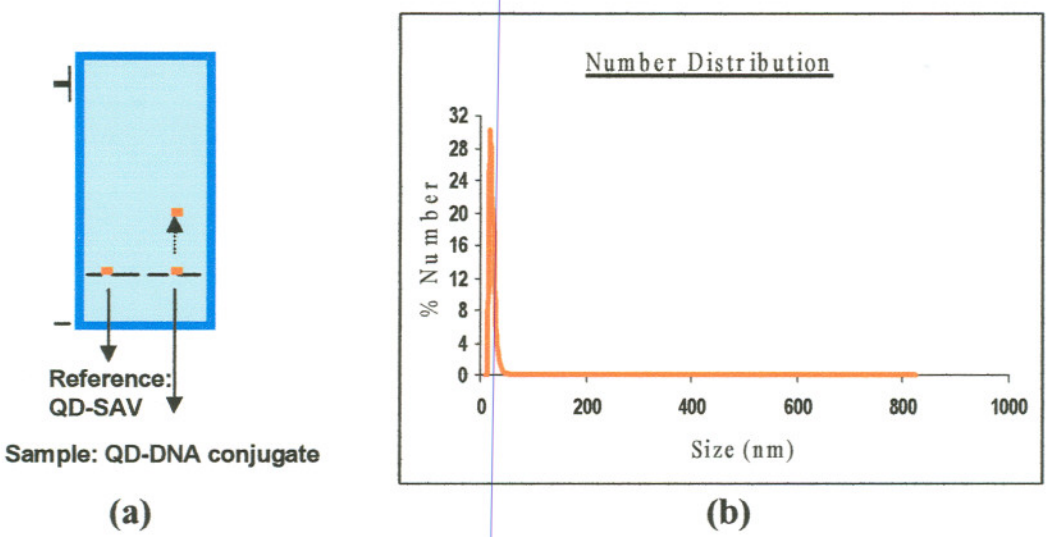

Figure 10. Characterization of QD-DNA conjugates. Part (a) represents a scheme of the QD-DNA movement along the chamber and part (b) shows that the Number distribution of the QD bioconjugated is 18 nm.

II. Photostability experiments

2. Laser Set up:

PROCEDURE

The laser set up is shown below in **figure 11.** The pump along with REGA generates a monochromatic laser beam of 800 nm, which is amplified by OPA to 400 nm. This more energetic laser beam split into two paths, one which serves as the reference beam, and the other one (probe beam), which goes through the sample. Both, reference beam and the probe beam are captured by the two APD's (Avalanche Photodiode). The two APD's transfer the signal separately to a box car integrator, which calculates the intensity and sends the data to PC. The data is recorded in a Spectra-Sense software.

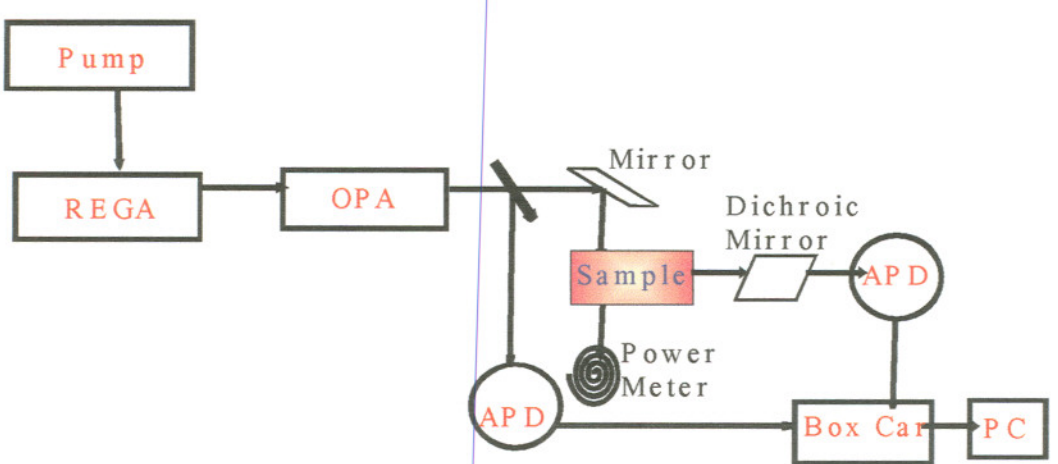

Figure 11. The experimental laser set up.

RESUTLS AND DISCUSSION

To carry out the laser experiments, the samples are previously diluted five times in ultrapure water, keeping equivalent concentrations in all the samples, and sonicated during several hours. A quartz cuvette is used for the experiment. The laser is set up at 89 mW (initial power). The initial power passing through the sample is71 – 74 mV. The exposure time is 25 minutes. In some of the cases, the power increased during the irradiation, between 3 to 4 power units. This phenomenon is attributed to annealing effects.[10, 11, 12] The spectra of power intensity as a function of time for the QD- micelles with different PEG lengths (**12a, b, c, d, e**) and the QD-DNA conjugate (**12f**) were recorded and compared to bare ZnS/CdSe nanoparticles (**12g**), refer to **figure 12.**

The objective of irradiate different sizes of micelles-QD's was to see if there is any effect on the mobility of the reactive species (water, oxygen) through the lipid coating. The results shown in **figure 12** indicate a similar decay rate for all the PEG lengths. In addition, these results are comparable to decay rate for avidin-biotin-DNA length. Therefore, it seems that the thickness of the lipid layer does not influence the photodegradation rate. This means that the micelle coating is not impermeable to the reactive ions, originated as a consequence of photochemical reactions.

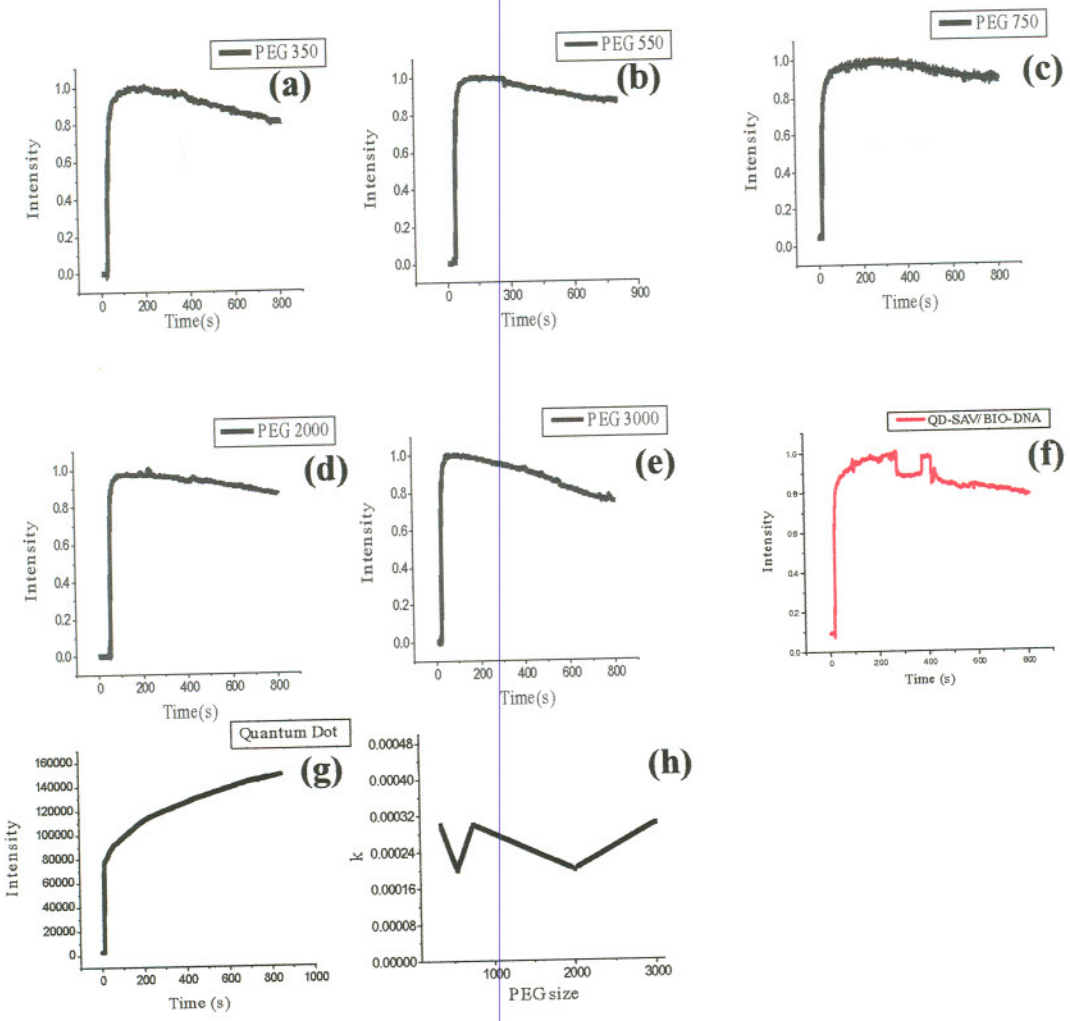

Figure 12. Laser results on different lengths of PEG and DNA coating on QD's.

A possible explanation for these results it supported by the belief that the lipid chain organizes as an amorphous polymer, which in turn increases the steric hindrance giving result to a free pathway for the ions to get in contact with the QD surface. For these set of experiments, it is obvious that the PEG length does

not influence in the QD stability, refer to **figure 12h** . Based on these results, a disordered polymer coating around the QD's was studied, the selection was the QD-DNA conjugate. The laser experiment on this sample provides evidence that the functionalization of the QD's with avidin-biotin linkage offers the same photostability as the micelle-QD's. Finally, the fluorescence spectroscopy of the exposed samples showed an increment of four times in the intensity with no shift compared to the unexposed samples, which is in perfect agreement with the literature, as shown in **figure 13**.

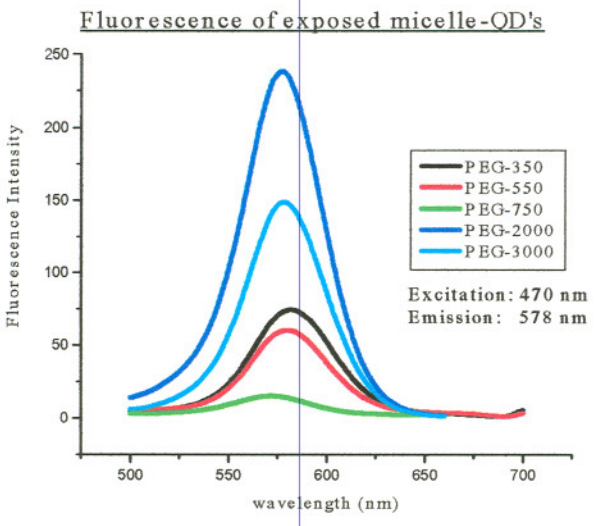

Figure 13. Emission intensity of the exposed samples.

CONCLUSIONS AND FUTURE WORK

One important conclusion derived from the laser experiments is that the decay rate is almost the same for all the PEG lengths. Therefore the size of the PEG length does not affect the photostability of the QD. Moreover, micelle-QD and QD-DNA show similar photoreactivity, thus, either of these two systems can be used to perform phototoxicity studies on QD's. The content of Cadmium ions released in solution can be monitored by ICP. In the case of the micelles, the PEG-350 will be chosen to carry out the ICP experiments. The final result from these analyses will determine if the micelle can be incorporated inside the BMV virus capsid.

REFERENCES

1. Michalet, X; Pinaud, F. F; Bentolila, L.A; Tsay, J. M; Doose, S; Li, J. J; Sundaresan, G; Wu, A. M; Gambhir, S.S; Weiss, S. *Science*. **2005,** 307, 538-544.
2. Maxwell, D. J.; Taylor, J. and Nie, S. *J. Am. Chem. Soc*. **2002,** 124, 9606-9612.
3. Schmid, G. "Nanoparticles" Wiley-VCH, 2004, pg 29-31.
4. Schmid, G. "Nanoparticles" Wiley-VCH, 2004, pg 61-85.
5. Quantum Dot Streptavidin Conjugates User Manual, PN 90-0003, Rev 9.2.
6. Pinaud, F; King, D; Moore, H-P; Weiss, S. *J. Am. Chem. Soc.* **2004,** 126, 6115-6123 9.
7. Dubertret, B; Skourides, P; Norris, D.J; Noireaux, V.; Brivanlou, A.H; Libchaber, A; *Science* **2002,** 298, 1759-1762.
8. Chen, C; Kwak, E-S.; Stein, B; Kao, C; Dragnea, B. Submitted to *Advanced Materials*, **2004**
9. Cordero, S. R; Carson, P. J; Estabrook, R. A; Strouse, G. F; Buratto, S. K. *J. Phys. Chem. B* **2000**, 104, 12137-12142.
10. Manna, L; Scher, E. C; Li, L-S; Alivisatos, P. A. *J. Am. Chem. Soc.* **2002,** 124, 7136-7145.

11. Leatherdale, C. A; Bawendi, M. G. *Physical Review B.* **2001,** 63, 165315-1 – 165315-6.

12. Bol, A. A; Meijerink, A. *J. Phys. Chem. B.* **2001,** 105, 10203-10209.

13. Jovin, T. M; *Nature Biotechnology* **2003,** 21, 32-33.

14. Bruchez, Moronne, Gin, Weiss, Alivisatos, P. A. *Science,* **1998,** 281, 2013.

15. West, J.L. and Halas, N.J. *Current opinion in Biotechnology* **2000,** 11, 215-217

16. Margaret A. Hines and Philippe Guyot-Sionnest *J. Phys. Chem* **1996,** 100,468-471

17. Chan, W. C; Nie, S. M. *Science,* **1998,** 281, 2016

18. Kim, S; Bawendi, M. G. B. *J. Am. Chem. Soc*, **2003,** 125, 14652.

19. Guo, W; Li, J-J, Wong, Y. A; Perg, X. G *Chem. Mater* **2003,** 15, 3125

20. Miyawaki, A; Savano, A; Kogure, T *Imaging in Cell Biology*, **2003,** 51-57.

21. Goldman, E. R; Balighian, E. D; Mattoussi, H; Kuno, M. K; Mauro, J. M; Tran, P. T; Anderson, J. P. *J. Am. Chem. Soc,* **2002,** 124, 6378-6382

22. Belsito, S; Bartucci, R; Montesano, G; Marsh, D; Sportelli, L; *Biophysical Journal*, **2000,** 1420–1430

23. Troutier, A-L; Delair, T; Pichot, C and Ladavie`re, C. *Langmuir* **2005,** *21,* 1305-1313

24. Johnson, M.;Hansson, P; Edwards, K; *J. Phys. Chem. B.* **2001,** 105, 8420-8430.

25. Hristova, K. and Needham D; *Macromolecules* **1995**, 991-1002.